

## Characteristics of wet-spun and thermally treated poly acrylonitrile fibers

Martin Kirsten,<sup>1</sup> Juliane Meinl,<sup>2</sup> Katrin Schönfeld,<sup>3</sup> Alexander Michaelis,<sup>4</sup> Chokri Cherif<sup>5</sup>

<sup>1</sup>Technische Universität Dresden/Institute of Textile Machinery and High Performance Material Technology, Breitscheidstr. 78, Dresden 01237, Germany

<sup>2</sup>Fraunhofer-Institut Für Keramische Technologien Und Systeme IKTS/Thermal Analysis and Thermal Physics, Winterbergstraße 28, Dresden 01277, Germany

<sup>3</sup>Fraunhofer-Institut Für Keramische Technologien Und Systeme IKTS/Nitride Ceramics and Structural Ceramics with Electrical Function, Winterbergstraße 28, Dresden 01277, Germany

<sup>4</sup>Fraunhofer-Institut Für Keramische Technologien Und Systeme IKTS, Winterbergstraße 28, Dresden 01277, Germany

<sup>5</sup>Technische Universität Dresden/Institute of Textile Machinery and High Performance Material Technology, Hohe Str. 6, Dresden 01069, Germany

Correspondence to: M. Kirsten (E-mail: martin.kirsten@tu-dresden.de)

**ABSTRACT:** The performance of carbon fibers depends on the quality of the precursor and the conditions of the thermal treatment. In detail, for a PAN precursor fiber the viscosity of a spinning dope and the draw ratio during the spinning process needs to be considered. Through wet spinning, different types of PAN precursor fibers with defined spinning parameters, including solid content, solvent content in a bath, and especially draw ratio resulting in defined cross section diameters, were fabricated and analyzed with tensile tests, density investigations, SEM, TGA-MS, FTIR, and XRD. The results show that the mechanical properties of the fibers correlate to crystallinity. The cross section diameter is strongly related to the morphology of the fibers after thermal treatment. By extending the postdrawing of PAN fibers high tenacities were obtained at the cost of the cross section shape. In addition, TGA measurements reveal trapped residues of the wet spinning process as well as show several chemical reactions takes place at the same time at different temperatures. © 2016 Wiley Periodicals, Inc. *J. Appl. Polym. Sci.* **2016**, *133*, 43698.

**KEYWORDS:** crystallization; fibers; mechanical properties; structure–property relations; thermal properties

Received 14 January 2016; accepted 26 March 2016

DOI: 10.1002/app.43698

### INTRODUCTION

The steady growth of world population leads to a significant increased demand for energy, water, food, clothing, communication, and mobility. Under the aspect of the global tendencies like demographic changes, migration, urbanization, economic development, and environment new technologies and materials are required. The mobility of individualized lifestyles thereby represents a major challenge for the research and development of the 21st century.

Herein, the modern lightweight construction with carbon fibers offers a key technology to reduce the moving mass. Poly acrylonitrile (PAN) has established itself in the last decades as a suitable precursor for carbon fibers and it is expected that the PAN will keep position in the market for the next years.<sup>1</sup> Nearly 90% of the carbon fiber in the world is made from poly acrylonitrile precursor. There are a lot of studies in literature dealing with the wet-spinning of PAN.<sup>2–7</sup> The quality of the carbon fibers

and thus the components made from it can be highly influenced by the properties of the precursor<sup>8</sup> and its process parameters of thermal treatment. The quality of the precursor can be specifically adjusted by different process parameters.<sup>9,10</sup> The orientation of the polymer chains, the failures in form of voids and cracks (Figure 1) in the structure of the fibers as well the cross section and the evenness of the PAN fibers has an important role to define the properties of the final products.<sup>1,8</sup> The production of carbon fibers is a complex process, which is just controllable through the deep understanding of many parameters, e.g., force of tension during treatment, dwelling times and temperature gradients.<sup>1</sup>

The PAN precursor is usually dissolved in a suitable organic polar solvent (e.g., dimethyl formamide—DMF, dimethyl acetamide—DMAc or dimethyl sulfoxide—DMSO) and then spun to endless filaments. In the wet-spinning process, which is the preferred process for high-strength fibers nowadays, the spin dope

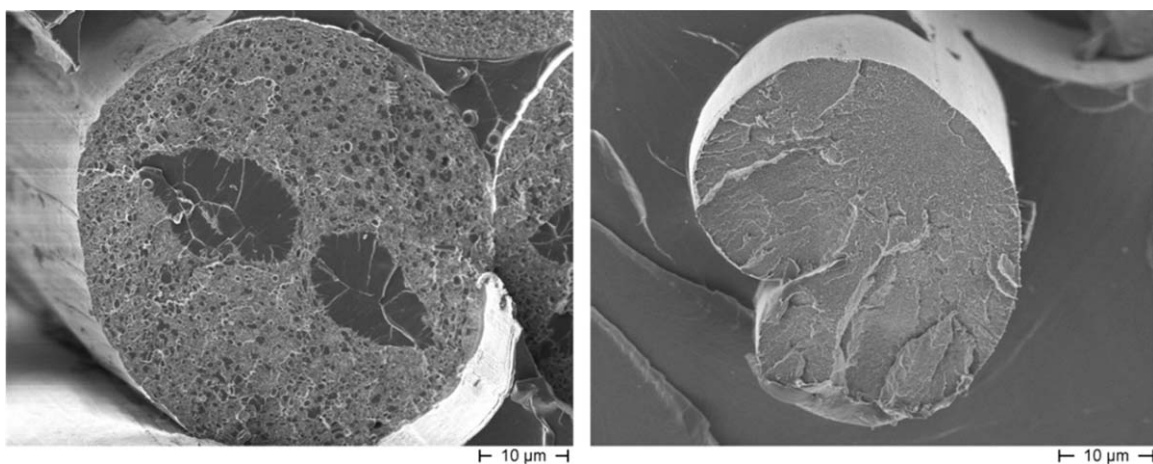


**Figure 1.** SEM image of wet spun PAN fibers showing large voids (left) and kidney shape like structure (right).

is forced through a spinneret with a specific number of holes into a coagulation liquid and then stretched and washed a couple of times.<sup>1</sup> A low coagulation rate is preferred to avoid defects inside the fibers as well as on the surfaces.

A low coagulation rate can also prevent the formation of the skin-core structure.<sup>8</sup> The gel-state, which is caused by the high concentration of solvent in the coagulation bath, facilitates the orientation of the polymer chains.<sup>8</sup> Further increase in tensile properties is observed after the washing baths, where the molecular orientation increased.

After the spinning of PAN filaments follow the crucial steps of heat treatment, namely stabilization and carbonization. For high

mechanical properties of carbon fibers, it is important to apply tension towards the PAN fiber during the thermal treatment. Linear PAN has polar nitrile groups in the molecules, resulting in strong intermolecular interactions, which leads to a high melting point of the PAN and, therefore it degrades respectively converts before its melting point. The intrinsic property of strong intermolecular interactions and ability to crystallization is the point of departure for the thermal treatment.<sup>8</sup> However the solubility of PAN is influenced, hence some other comonomers are incorporated weaken the intermolecular interactions. Thus, not only the solubility but also the handling during stabilization of PAN can be improved. Several studies stated the improvement in the carbon fiber mechanical properties due to

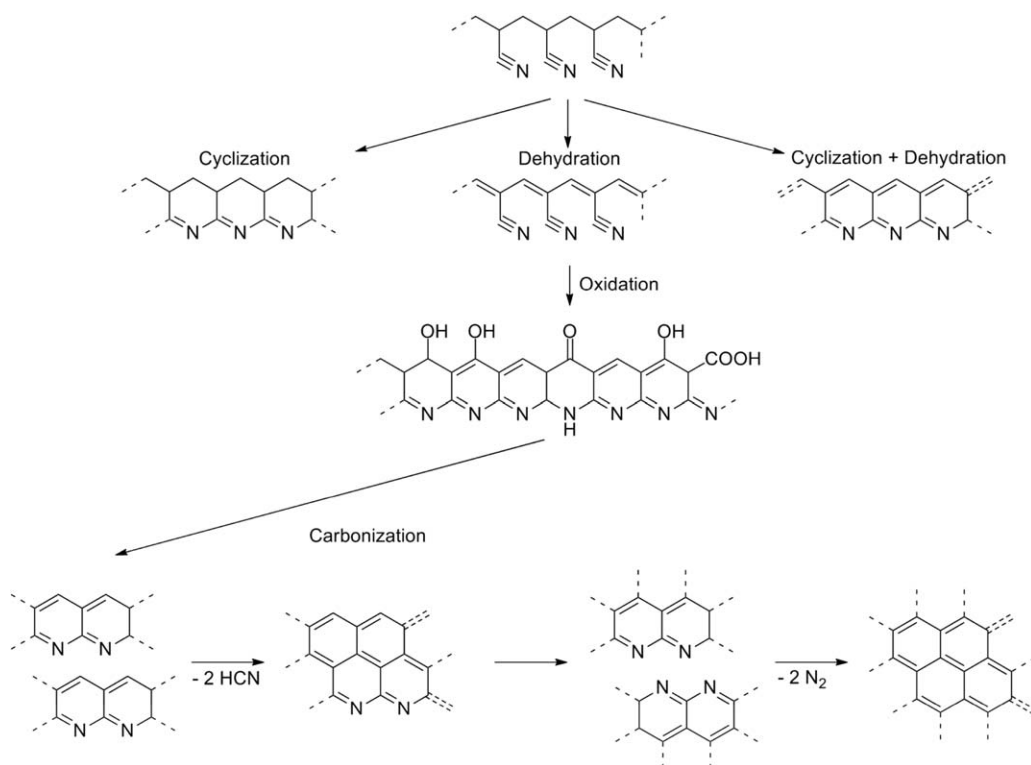


**Figure 2.** Process of carbon fiber formation starting from PAN.<sup>11</sup>



**Figure 3.** Wet-spinning pilot plant by Co. Fourné Polymertechnik GmbH, Germany. [Color figure can be viewed in the online issue, which is available at [wileyonlinelibrary.com](http://wileyonlinelibrary.com).]

the increased molecular orientation in precursor fibers and the resultant carbon fibers.<sup>8</sup>

The stabilization, which includes cyclization and dehydration (Figure 2), is performed at temperatures up to 300 °C in an oxidizing atmosphere, preferably air. The nitrile groups undergo cyclization, which is highly exothermic and has to be controlled by adjusted process conditions, especially low heating rates, making the stabilization process very time consuming. In this step, the smaller the PAN diameter, the better is the stabilization. So, the exothermic reaction is more controllable with smaller sized fibers.<sup>1,8</sup> The resulting oxidized PAN has a partially aromatic ladder structure and contains oxygen functional groups (Figure 2), it is inflammable and infusible and therefore suited for the high temperature treatment. Afterwards the thermally stabilized and oxidized fiber can be heated above 600 °C without burning. At such temperatures, the processes of decyanization and dehydrogenation as well the removal of nitrogen take place, followed by formation of large aromatic sheets at 1300 °C. Throughout the production the weight loss is approximately 50%. This leads to failures in the structure (longitudinal voids).<sup>1</sup>

Mainly two facts distinguish the final properties of a carbon fiber, namely the choice of the precursor material and the process parameters of conversion starting from the PAN precursor fiber ending up with the carbon fiber. The critical cross section diameter to be achieved is 12–13 μm. The tensile strength of the precursor fibers has to fit the processing properties of following thermal treatment steps. This goes along with a pre-oriented polymer structure in fiber direction. The quality of the precursor has to be validated by different characterization meth-

ods, e.g., density measurements, cross section—SEM analysis, FT-IR, tensile, and XRD measurements and adjusted towards the process parameters of wet spinning.<sup>6,12–21</sup>

The knowledge about the carbon fiber production including all steps starting with spinning PAN precursor fibers in its thermal treatment is well protected and limited to big players in this field of business. Therefore, it is an urgent need to investigate comprehensively the precursor spinning as well as the thermal treatment looking prospectively towards pilot plant scale.

## ANALYSIS

IR spectra were obtained by using the Attenuated Total Reflection method on a Bruker Tensor 27 FTIR spectrometer. A total of 32 scans were taken and averaged from 400 to 4000  $\text{cm}^{-1}$  with a resolution of 4  $\text{cm}^{-1}$  for each spectrum.

Thermal Gravimetric Analysis (TGA) was carried out on a STA 449C (NETZSCH-Gerätebau GmbH) in air with a flow rate of 5 l/h and a heating rate of 2 K/min. Thermal Gravimetric Analysis coupled with Mass Spectrometry Emission Gas Analysis (TGA-MS) was carried out on a STA 429 with a SKIMMER coupling system 403/3 (NETZSCH-Gerätebau GmbH) and a quadrupole mass spectrometer QMG 422 (Balzers) in an helium-oxygen atmosphere with a flow rate of 5 l/h. The heating rate was 5 K/min.

Tensile properties of the PAN yarn samples were measured according to DIN EN ISO 2062 on a Z2.5 tensile tester (Zwick, Germany) with a 100 N load sensor. The gauge length was 250 mm and the extension rate was 250 mm/min. The tests were

**Table I.** Mechanical Properties of Selected PAN Fibers

Fiber type	Draw ratio (overall)	Cross section diameter (μm)	Tenacity (cN/tex)	Young's modulus (GPa)
Not drawn				
1	1:3.0	18.4	9.4	5.7
2	1:5.9	16.0	20.6	7.2
Thermally Postdrawn				
3	1:10.9	13.0	48.1	17.2
4	1:10.7	13.9	42.0	16.6
5	1:12.3	–	60.8	15.4

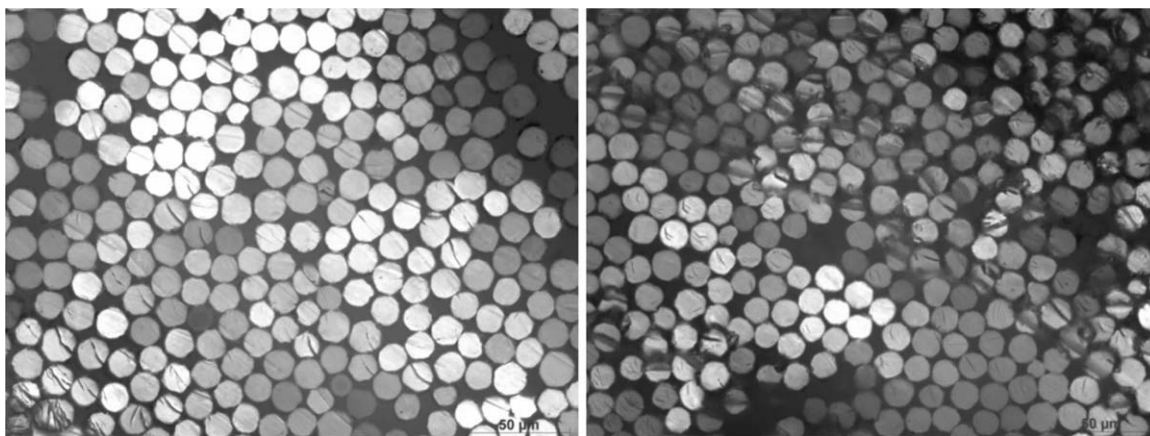


**Figure 4.** Cross sections of PAN precursor (4) before (left) and after (right) drawing.

performed at 20 °C, 65% relative humidity. The tensile tests were carried out on 10 samples of each fiber quality, the standard deviation being generally less than 5%.

The density of fibers was determined with mercury porosimetry on Autopore IV 9500 equipment using 0.1 g material.

X-ray diffraction (XRD) analysis was examined at Bruker D8 diffractometer with PSD (position sensitive detector) and  $\text{CuK}\alpha$  irradiation on fiber bundles. The scan angle ranged from 10° to 60° in 0.02° step width.

Cross sections were prepared in order to prove the shape and the cross section diameter of the spun yarn. A yarn was cut using a razor blade and analyzed via light microscopy.

Scanning electron microscopy was performed to obtain the microstructure via cross section of the fibers which were analyzed on ceramic graphically on SEM Leica S260.

## EXPERIMENTAL

### Wet-Spinning of PAN Fibers

The spinning dope solution was prepared using up to 23 wt % of PAN ( $M_w$  200,000 g/mol) in dimethyl formamide (DMF) the viscosity of the spin dope was optimized through appropriate temperature elevation. The solution was filtered through a candle

filter system and stirred for 5–10 h. Subsequently it was degassed under vacuum. Spinning nozzles with 1000 holes and a single filament cross section diameter of 120  $\mu\text{m}$  were used. The spinning was conducted on a wet-spinning pilot plant by Fourné Polymertechnik GmbH, Germany (Figure 3) consisting of one coagulation (Solvent composition DMF 85%, water 15%), three washing baths, one drying and sizing unit and a winder with an overall speed of up to 60 m/min. The storage tanks of the washing baths are independent from each other having different solvent concentrations and temperatures. The postdrawing improving the mechanical and structural properties of the PAN precursor was performed on a pilot plant scale postdrawing unit by DIENES Apparatebau GmbH, Germany where the yarn is transported and heated by duos of godets. The heat was transferred by direct contact into the fiber. The overall speed was up to 25 m/min depending on the drawing ratio. In this paper, the overall drawing ratio was calculated assuming a constant mass throughput of PAN, starting from the extrusion of the spin-dope in relation to the take up speed at the winder is meant.

### Thermal Treatment—Oxidation and Carbonization

The oxidation was done in a Carbolite CTF tube furnace through which the fiber bundle was pulled by a Mikrosam MAW20-LS1 winding machine, allowing for a constant fiber

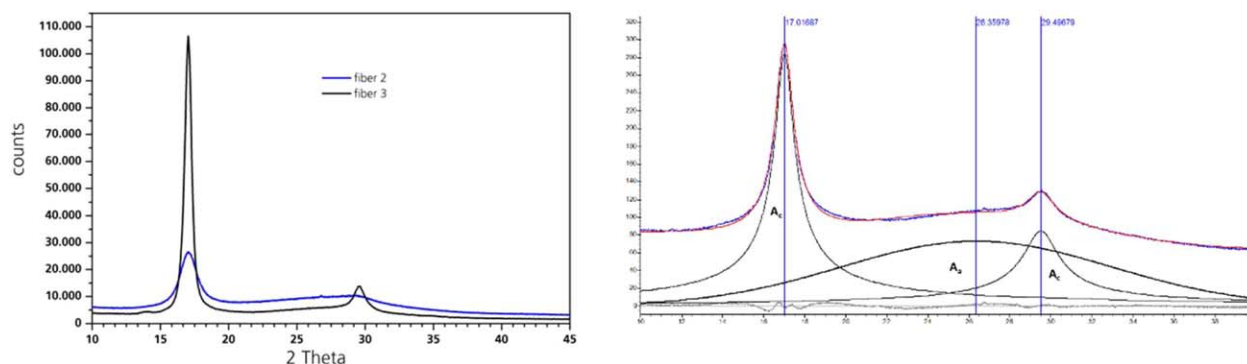


**Figure 5.** XRD pattern of PAN fiber with and without stretching during spinning process (left) and schematic representation of extrapolation of crystalline and amorphous components in XRD pattern of PAN according Gupta<sup>25</sup> (right). [Color figure can be viewed in the online issue, which is available at wileyonlinelibrary.com.]

**Table II.** Characteristic of XRD for the Selected PAN Fibers

	2 $\theta$ (°)	Peak area	Crystallinity (DO)
Nondrawn PAN	17.0743	546.29	0.37
	26.4526	1562.45	
	29.2639	388.09	
Drawn PAN	17.03179	1003.16	0.64
	26.8714	835.57	
	29.54776	511.70	

tension during the process. The furnace was open and air was passed through the tube while the fiber bundle was continuously running with a defined speed. The carbonization was done under static conditions with a TT2 oven (Thermal technology GmbH) with graphite heater and crucible and nitrogen atmosphere.

## RESULTS AND DISCUSSION

Several physical, chemical, and mechanical challenges concerning the final fiber properties had to be addressed and solved. In detail, the solution viscosities, spin stretch (draw) ratio (ratio of take-up speed to extrusion rate) adjustment, coagulation bath regulation and drying methods are some of the parameters which urgently need to be thermally examined and regulated. A defined temperature gradient of the dope and the coagulation bath for the production of homogeneous fibers free of voids is necessary. For a better understanding and reliable benchmark, stabilization, oxidation, and carbonization of the wet-spun fibers are performed and characterized. Although, copolymers of PAN are in the focus of current research and investigation, a homopolymer of PAN was chosen for the experiments to set up the preconditions of understanding the mechanisms of structure formation of PAN fibers and the resulting structure–property relation.

### Wet Spinning of PAN Precursor Fibers and Postdrawing

The mechanical properties (Table I) indicate the quality of the fiber due to orientation of the polymer chains into fiber direction. For fiber type 1, it can be stated, that a draw ratio of factor 1:3.0 during wet spinning leads to poor properties dealing with a tenacity of 9.4 cN/tex and a Young's modulus of 5.7 GPa. Adjusting the final diameter of the PAN precursor fibers, enormous changes go along with increasing the draw ratio. For fiber type 3, which originates from type 2 with 20.6 cN/tex, a

**Table III.** Density of Pan and Oxidized Fibers

Material	Density of PAN fiber material (g/cm <sup>-3</sup> )	Density of oxidized PAN fiber material (g/cm <sup>-3</sup> )
Reference (type R1) <sup>21,27</sup>	1.07–1.18	1.34–1.39
PAN without stretching (type 2)	0.95–1.05	1.30
PAN with stretching (type 4)	1.18	1.46

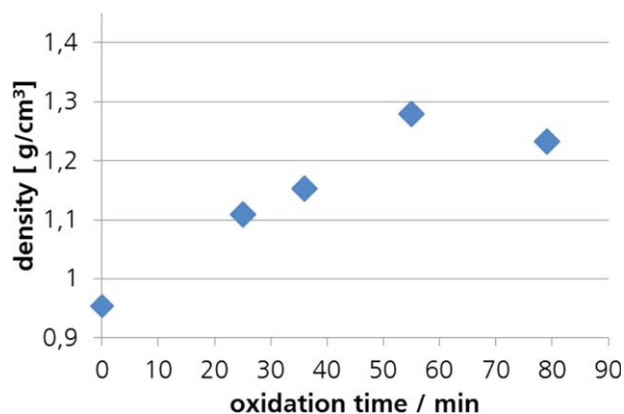


**Figure 6.** Increase of density of PAN fiber type 2 towards an oxidized fiber with time. [Color figure can be viewed in the online issue, which is available at wileyonlinelibrary.com.]

tenacity of 48.1 cN/tex was achieved by enhancing the stretching ratio from 1:5.9 to 1:10.9. By pushing towards to the limits of the process conditions, a yarn (type 5) was obtained with 60.8 cN/tex tensile strength. Unfortunately, the cross section shape of the fibers is not circle-like anymore but rather rectangular, probably due to the compression by high lateral forces between the filaments during the drawing.

Postdrawing of the PAN fibers is a crucial requirement to improve the mechanical properties as well as the orientation of the polymer chains in the fiber direction. Investigations relating to the correlation of the draw ratio and mechanical properties are very important for research as well as industrial applications. The experimental setup can be realized in various ways. It is beneficial to conduct the drawing at least at the glass transition temperature of PAN—approximately 95 °C. In all experiments shown in Table I, the stretching was performed at 140 °C turning 8 loops at each pair of godets. With higher temperatures, the reaction rate of the cyclization of nitrile groups increases leading to a nondrawn precursor material with poor properties, further useless for the conversion to carbon fibers. Therefore it has to be strictly controlled and kept in a small

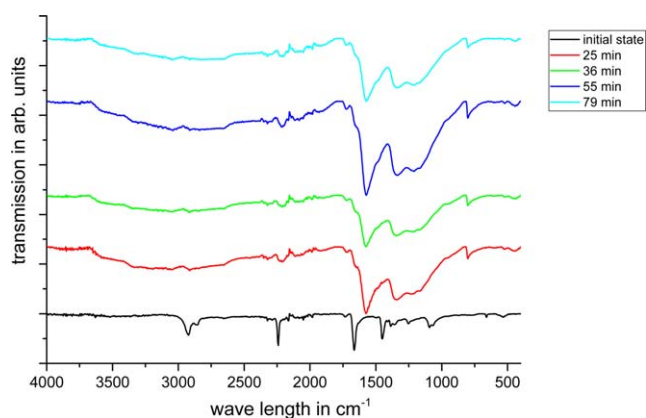


**Figure 7.** FTIR-spectra of fiber type 2 under thermal treatment with different oxidation durations. [Color figure can be viewed in the online issue, which is available at wileyonlinelibrary.com.]

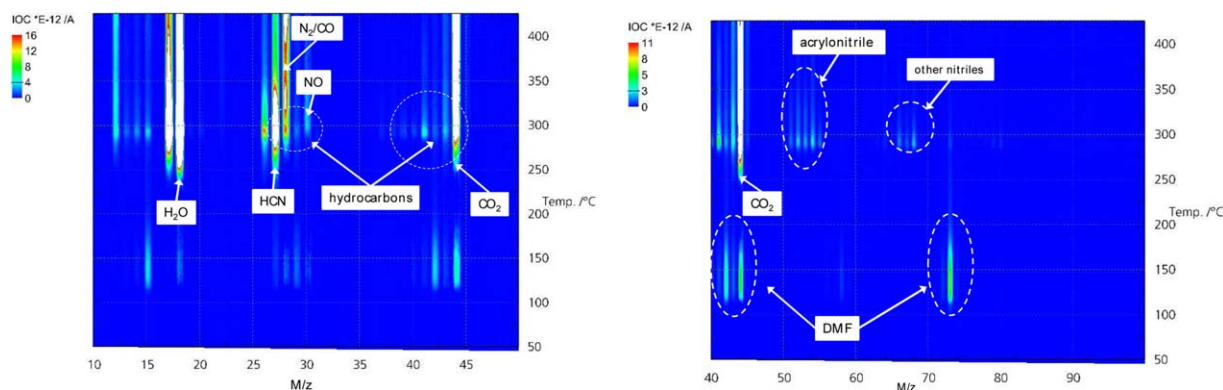


**Figure 8.** TGA-MS spectra of fiber type 2 revealing the loss of specific compounds at different temperatures. [Color figure can be viewed in the online issue, which is available at [wileyonlinelibrary.com](http://wileyonlinelibrary.com).]

process window in between 90 °C and 150 °C. Cross sections were examined to check the final properties, especially homogeneity, shape and diameter of single filaments. The comparison of fiber type 4 before and after drawing is shown in Figure 4. No significant change of shape can be observed. Additionally a homogenous distribution of diameters can be stated.

The improved mechanical properties are one indication of the structural changes of the fiber during the wet spinning as well the drawing process. Those findings are supported by XRD and fiber density measurements.

#### X-ray Diffraction—XRD

As mentioned before, the stretching process influences the morphology and the structure of the PAN fiber is significantly affected. After each process step the fibers were investigated with XRD measurements to obtain information about the degree of orientation and crystallization. A moderately sharp reflection in the region  $2\theta = 16^\circ$ – $17^\circ$ , which occurs as the equatorial reflection in oriented samples, a broad diffuse scattering maximum at higher diffraction angle, and a small diffraction peak around  $2\theta = 30^\circ$  are characteristic features of XRD pattern of PAN.<sup>22</sup> So PAN fibers can be described by the classical crystalline and amorphous structure model for semi crystalline polymers.<sup>23</sup> The reflection at about  $17^\circ$  is attributed to the crys-

talline structure by the protagonists<sup>22</sup> which corresponds to a planar spacing  $d = 5.240 \text{ \AA}$  indexed to the (100) plane of a hexagonal structure.<sup>24</sup> and the crystalline reflection at about  $29.3^\circ$  conforms to the second-order reflection of peak 1. The amorphous part is corresponding with the maximum at around  $2\theta = 26^\circ$  (Aa) However, the corresponding peak height or diffraction intensity varies with the various PAN fibers, which implies that they have different structures as it can be seen in Figure 5.

The degree of order— $DO = Ac/(Ac + Aa)$  or crystallinity was calculated according Gupta method.<sup>25</sup> The crystallinity of PAN is increased due to fiber stretching because of the alignment of polymer molecules of the PAN structure. The degree of order was higher than the reference fiber. In Table II, the development of the increasing crystallinity especially the degree of order is shown and can be calculated, respectively. It was nearly doubled and raised from 0.37 of nondrawn PAN towards 0.64 of a post-drawn precursor fiber. For a reference fiber from Mitsubishi Rayon (Japan) a crystallinity of 0.87 was measured which is good benchmark for comparing the experimental results.<sup>20</sup>

#### Density

The densities of the PAN fibers are specified in the literature with  $1.18 \text{ g/cm}^3$ .<sup>26</sup> For fibers without stretching (type 2) densities between  $0.95$  and  $1.05 \text{ g/cm}^3$  were obtained (Table III). After drawing the diameter of the fibers (Table I) was reduced by approximately  $5 \mu\text{m}$  and the density of the fibers increased, which is shown in Table III. Most of the pores and micropores vanish resulting in a more compact morphology. Especially for the fiber type 4 the same density as in the reference material was obtained by the process parameters of the wet-spinning process and the postdrawing.

During the oxidation process oxygen atoms are incorporated and intermolecular crosslinking of the PAN chains occurs. A preliminary network is created. Due to this molecular change in structure by chemical reactions and physical processes the density increases (Figure 6) and can be used to evaluate the structure of the oxidized material. In fiber 4, it results in a density of  $1.46 \text{ g/cm}^3$ , suggesting a highly ordered and dense PAN structure. The reference as well as the none-postdrawn fiber shows a

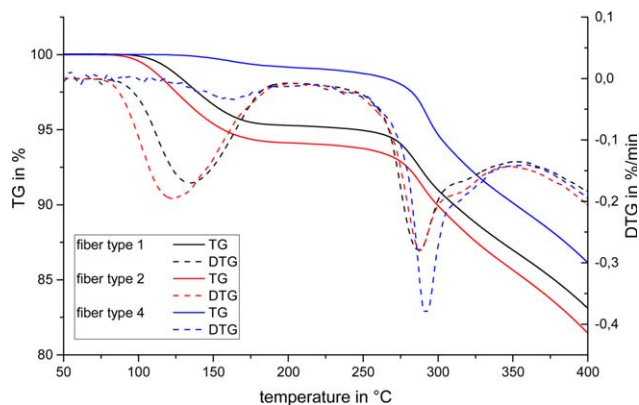


**Figure 9.** TG and DTG-curves of the fibers during oxidation treatment in air with a linear heating rate of 2 K/min. [Color figure can be viewed in the online issue, which is available at [wileyonlinelibrary.com](http://wileyonlinelibrary.com).]

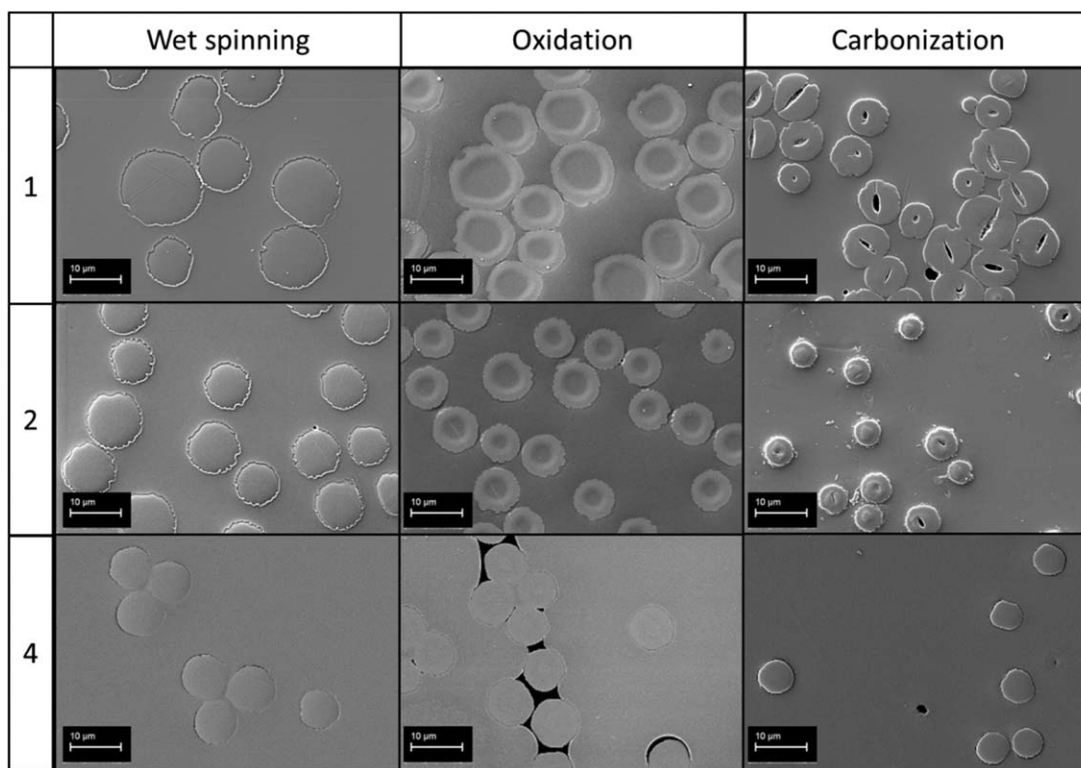


**Figure 10.** SEM cross sections of 1, 2, and 4 showing different morphologies.

lower density. Those findings are consistent with the results in literature.<sup>26</sup>

Besides the structure of the starting material, the parameters during thermal treatment mainly influence the density of the oxidized PAN material. The influence of the duration of oxidation treatment on the density was studied. The process was performed as described above. After an oxidation time of 80 min, a slight decrease in density was observed (Figure 6). The oxidized fiber reaches after 55 min its density maximum. This indicates chemical reactions inside the fiber, resulting in structural changes causes a decrease in density.

#### FTIR-Spectroscopy of Pristine and Oxidized Fibers

To achieve additional information about the structure and morphology of the obtained PAN-precursor fiber and its oxidized form, FTIR spectra (Figure 7) of the samples after different oxidation times have been investigated. The pristine polymer shows characteristic peaks of the aliphatic backbone (CH<sub>2</sub> stretching) and the nitrile groups (2240 cm<sup>-1</sup>). The cyclization and dehydrogenation during the thermal treatment can be seen by the disappearance of the aliphatic peaks and the nitrile peaks and the appearance of C=C—peak at 1572 cm<sup>-1</sup>. A small and broad peak at 2200 cm<sup>-1</sup> can be observed and is attributed to the formation of conjugated C=N structures. The oxidation leads to the formation of carbonyl groups (C=O at 1730 cm<sup>-1</sup>). The infrared spectra of fibers treated with different oxidation times show no significant differences. The origin PAN structure vanishes already after the shortest oxidation treatment. Further structural changes may not be visible in the infrared range.

#### Thermogravimetric Analysis—Mass Spectra (TGA-MS)

The stabilization step of the thermal treatment of PAN fibers is accompanied by a mass loss and a variety of gas emissions. The reactions are strongly influenced by the morphology of the precursor materials. Therefore thermogravimetric studies and emission gas analysis is a valuable tool to explore the influence of spinning parameters on the stabilization behavior of the fibers.

Regarding the investigated samples, the mass loss due to the stabilization reactions starts approximately at 250 °C. It results mainly from dehydrogenation processes and side reactions. While dehydrogenation leads to water emission, side reaction products appear in the form of cyanic acid, nitrous oxides or hydrocarbons (acrylonitriles and other nitrile compounds). The formation of cyanic acid (HCN) and ammonia (NH<sub>3</sub>) is also attributed to cyclization reactions, although an ideal reaction process would occur without mass loss.<sup>25,27,28</sup> Side reactions need to be kept at minimum, since they lead to a significant loss in carbon yield. The exothermic cyclization reactions during stabilization can lead to material overheating, which facilitates side reactions like chain scission and degradation, resulting in structural and morphological damages of the fibers. Therefore, the stabilization is performed at low heating rates to compensate the influence of the heat of reaction. As visible from the TG-MS results in Figure 8, the mass loss continues at higher temperatures in air, especially due to destructive oxidation processes and the resulting CO<sub>2</sub> formation. A prolonged oxidation time might therefore already lead to a degradation of carbon precursor material and is not beneficial to the structure formation. This effect might account for the density loss measured in the samples with prolonged oxidation time, as described above.

Residues of spinning solution which are trapped in the fiber pores can lead to the reduction of the mechanical properties of the resulting carbon fibers after thermal treatment, as it might lead to voids or structural damages when released. The thermogravimetric analysis of 1 and 2 in Figure 9 represented an additional mass loss in the range of 100–150 °C, which can be attributed to the emission of DMF through emission gas analysis in Figure 8. By optimizing the spinning and drawing process, the DMF residues in the fiber type 4 were noticeable reduced.

The mass loss in the stabilization step is also influenced by the processing parameters. With higher draw ratio, the mass loss during stabilization is increased. The DTG peak during the stabilizing changes to higher temperatures and shows a higher intensity. This might be correlated to the increased orientation of the fibers and the thereby enhanced crystallinity. It is assumed, that the stabilization are shifted to higher temperatures in crystalline regions of the polymer.<sup>29</sup> The crystallinity improves the interactions of the molecular structure, leading to higher onset temperatures, while the orientation increases the amount of molecular structures that can participate in the stabilization reactions.

Comparing the fiber types 2 and 3 during the TG-MS measurements, the influence of the draw ratio on the mass loss behavior can be seen as well. Additionally, the analysis of the gas emissions with TG-MS shows the similar increase of peak temperature and amount of emissions for several gaseous products. As mentioned before, those gas products have been attributed to different reactions during the stabilization process. The change due to different processing parameters can therefore not only be attributed to one type of reaction, but seems to influence all ongoing reactions during oxidative stabilization, side reactions included.

#### Scanning Electron Microscopy—SEM

The carbonization is the last step of a common carbon fiber production and will be discussed in a following paper in detail. Further thermal treatment, namely the graphitization, can be conducted to improve the mechanical properties due to an enhanced orientation of the graphitic layers. At least in this paper, passing all process steps the quality of fibers was inspected at cross section (Figure 10) where the carbonization was. In the first row the PAN fibers without drawing at the beginning of the process optimization are shown. For this type of fibers after oxidation a two zone structure is clearly visible (1 and 2). This is due to incomplete cross linking of the PAN lattice in dependency on dwell time, temperature but also on the enlarged cross section diameter of the fiber. In the outer zone, the cross linking took place while in this area the material has a much higher density than in the middle of the fiber. Paulauskas *et al.*<sup>30</sup> proposed an appropriate mechanism in literature explaining these findings. Due to the difference in density of the cross section the fibers show structural defects such as holes and scratches after the carbonization. The kind of shrinkage during carbonization and the resulting morphology goes along with the inhomogeneous differences in density resulting into holes inside the fibers (fiber 1). In the next step (fiber 2) the diameter of the PAN fibers was reduced to 16.0 μm (Table I) by increasing of the stretching during spinning. The two-zone structure after oxidation is still visible but

regarding to the smaller cross section diameter after carbonization only a few fibers have holes inside. Further changes of the process parameters, especially the conducting of postdrawing lead to homogenous fibers (4) bypassing respectively avoiding the two zone morphology.

#### CONCLUSIONS

An attempt of obtaining suitable properties of wet-spun poly acrylonitrile fibers in pilot plant scale related to the thermal treatment towards the formation of carbon fiber was done. In this study, the wet-spinning process including the postdrawing was investigated in order to compare the information about the morphology and structure as well as physical properties and mechanical properties without affecting the cross section of the spun fiber. There is a significant influence of the orientation and alignment of the PAN along the fiber axis towards tensile strength. An aspect which absolutely needs to be regarded is the cross section diameter due to the dwelling time of thermal treatment. Two-zone morphology resulted into a kind of hollow fibers with so far not suitable properties after carbonization. Finally, adjusting the parameters, e.g., draw ratio, a PAN-precursor fiber was obtained, supported by XRD and density measurements, meeting the criteria for carbon fiber production. Information about the loss of mass at certain temperatures revealed trapped DMF in the fiber, which needs to be avoided completely at least by improving the wet-spinning process in ongoing investigations. Further research and development concerning the mechanism of fiber formation, stabilization, oxidation, and carbonization have to be studied intensively for a comprehensive understanding of the carbon fiber formation starting with the precursor development especially under the aspect of using alternative precursors such as lignin having more complex and irregular starting structure.

#### ACKNOWLEDGMENTS

The authors gratefully acknowledge the financial support by the European Union (EFRE) and Freistaat Sachsen (SAB EFRE 100062605).

#### REFERENCES

1. Ellringmann, T.; Wilms, C.; Warnecke, M.; Seide, G.; Gries, T. *Tex. Res. J.* **2015**, *0*, 1.
2. Yi, K.; Li, Q. F.; Li, L. Z.; Zhou, Y.; Ryu, S. K.; Jin, R. G. *J. Eng. Fiber Fabric* **2013**, *8*, 107.
3. Dong, X.; Wang, C.; Juan, C. *Polym. Bull.* **2007**, *58*, 1005.
4. Wang, Y.; Wang, C.; Bai, Y.; Bo, Z. *J. Appl. Polym. Sci.* **2007**, *104*, 1026.
5. Wilms, C.; Seide, G.; Gries, T. *Chem. Eng. Trans.* **2013**, *32*, 1609.
6. Ribeiro, R. F.; Pardini, L. C.; Alves, N. P.; Brito Júnior, C. A. *Polímeros* **2015**, *25*, 523.
7. Kalabin, A. L.; Pakshver, E. A.; Kukushkin, N. A. *Theor. Found. Chem. Eng.* **1996**, *30*, 295.
8. Huang, X. *Materials* **2009**, *2*, 2369.



9. Knudsen, J. P. *Tex. Res. J.* **1963**, 33, 13.
10. Hersh, S. P.; Higgins, T. D.; Krause, H. W. *J. Appl. Polym. Sci.* **1963**, 7, 411.
11. Cherif, Ch.; Freudenberg, C. In *Textile Werkstoffe für den Leichtbau—Techniken—Verfahren—Materialien Eigenschaften*; Cherif, Ch., Eds.; Springer: Berlin, **2001**; Vol. 1, Chapter 3.3.3.1, pp 74–78.
12. Vyazovkin, S *Anal. Chem.* **2006**; 78, 3875.
13. Widmann, J. DSC-Kurven interpretieren Teil 1: Dynamische Messungen; METTLER TOLEDO GmbH: Schweiz, **2000**; 1.
14. Widmann, J. DSC-Kurven interpretieren Teil 2: Isotherme Messungen; METTLER TOLEDO GmbH: Schweiz, **2000**; 2.
15. Anghelina, V. F.; Popescu, I. V.; Gaba, A.; Popescu, I. N.; DESPA, V.; Ungureanu, D. *J. Sci. Arts* **2010**, 12, 89.
16. Liu, X. D.; Ruland, W. *Macromolecules* **1993**, 26, 3030.
17. Lee, S.; Kim, J.; Ku, B. C.; Kim, J.; Joh, H. I. *Adv. Chem. Eng. Sci.* **2012**, 2, 275.
18. Eslami Farsani, R.; Raissi, S.; Shokuhfar, A.; Sedghi, A. *World Acad. Sci. Eng. Technol.* **2009**, 50, 430.
19. Karacan, I.; Erdogan, G. In *Fibers and Polymers*; **2012**, 13, 855.
20. Wangxi, Z.; Gang, L. J. W. *Carbon* **2003**, 41, 2805.
21. Zhang, W.; Li, M. *J. Mater. Sci. Technol.* **2005**, 21, 581.
22. Gupta, A. K.; Singhal, R. P. *J. Polym. Sci. Polym. Phys.* **1983**, 11, 2243.
23. He, D.; Wang, C.; Bai, Y.; Zhu, B. *J. Mater. Sci. Technol.* **2005**, 21, 376.
24. Ge, H.; Liu, H.; Chen, J.; Wang, C. *J. Appl. Polym. Sci.* **2009**, 113, 2413.
25. Grassie, N.; McGuchan, R. *Eur. Polym. J* **1971**, 7, 1357.
26. Jäger, H.; Hauke, T. In *Carbonfasern und ihre Verbundwerkstoffe: Herstellungsprozesse, Anwendungen und Marktentwicklung*; Jäger, H., Hauke, T., Eds.; Verlag Moderne Industrie GmbH: Landsberg, **2010**; Vol. 1, p 13.
27. Bajaj, P.; Sreekumar, T. V.; Sen, K. *Polymer* **2001**, 42, 1707.
28. Rahaman, M. S. A.; Ismail, A. F.; Mustafa, A. *Polym. Degrad. Stab.* **2007**, 92, 1421.
29. Sen, K.; Bajaj, P.; Sreekumar, T. V. *J. Polym. Sci. Polym. Phys.* **2003**, 41, 2949.
30. Paulauskas, F.; Naskar, A. K.; Bonds, T. A. Pat. Pub. No. U.S. 2012/0322332 A1.